J|A|C|S ARTICLES

Published on Web 03/04/2010

Organelle-Targetable Fluorescent Probes for Imaging Hydrogen Peroxide in Living Cells via SNAP-Tag Protein Labeling

Duangkhae Srikun,[†] Aaron E. Albers,[†] Christine I. Nam,[†,‡] Anthony T. Iavarone,[§] and Christopher J. Chang*[,†,‡]

Department of Chemistry and the Howard Hughes Medical Institute, University of California, Berkeley, California 94720, and QB3/Chemistry Mass Spectrometry Facility, Berkeley, California 94720

Received January 6, 2010; E-mail: chrischang@berkeley.edu

Abstract: Hydrogen peroxide (H_2O_2) is a potent small-molecule oxidant that can exert a diverse array of physiological and/or pathological effects within living systems depending on the timing and location of its production, accumulation, trafficking, and consumption. To help study the chemistry and biology of this reactive oxygen species (ROS) in its native cellular context, we now present a new method for monitoring local, subcellular changes in H_2O_2 levels by fluorescence imaging. Specifically, we have exploited the versatility of the SNAP-tag technology for site-specific protein labeling with small molecules on the surface or interior of living cells with the use of boronate-capped dyes to selectively visualize H_2O_2. The resulting SNAP-Peroxy-Green (SNAP-PG) probes consist of appropriately derivatized boronates bioconjugated to SNAP-tag fusion proteins. Spectroscopic measurements of the SNAP-PG constructs confirm their ability to detect H_2O_2 with specificity over other biologically relevant ROS. Moreover, these hybrid small-molecule/protein reporters can be used in live mammalian cells expressing SNAP-tag fusion proteins directed to the plasma membrane, nucleus, mitochondria, and endoplasmic reticulum. Imaging experiments using scanning confocal microscopy establish organelle-specific localization of the SNAP-tag probes and their fluorescence turn-on in response to changes in local H_2O_2 levels. This work provides a general molecular imaging platform for assaying H_2O_2 chemistry in living cells with subcellular resolution.

Introduction

Reactive oxygen species (ROS) derived from the metabolism of oxygen by living organisms are classically known as indicators for oxidative stress and potential contributors to aging[1−6] and diseases ranging from cancer[7−12] to diabetes[13−15] to neurodegeneration.[16−18] However, organisms that live in aerobic environments can also harness and incorporate ROS chemistry into their normal physiology by means of regulated production, release, and compartmentalization of these oxygen metabolites.[19−26] A prime example of ROS chemistry used for beneficial purposes is the oxidative burst within phagosomes of macrophages and neutrophils that serves as a defense against invading pathogens.[27−29] In this context, a major ROS produced in living systems is hydrogen peroxide (H_2O_2), which is a newly recognized messenger in cellular signal transduction but also a

[†] Department of Chemistry, University of California, Berkeley.
[‡] Howard Hughes Medical Institute, University of California, Berkeley.
[§] QB3/Chemistry Mass Spectrometry Facility.

(1) Harman, D. *J. Gerontol.* **1956**, *11*, 298–300.
(2) Finkel, T.; Holbrook, N. J. **2000**, *408*, 239–247.
(3) Stadtman, E. R. *Free Radical Res.* **2006**, *40*, 1250–1258.
(4) Droge, W.; Schipper, H. M. *Aging Cell* **2007**, *6*, 361–370.
(5) Muller, F. L.; Lustgarten, M. S.; Jang, Y.; Richardson, A.; Van Remmen, H. *Free Radical Biol. Med.* **2007**, *43*, 477–503.
(6) Sharpless, N. E.; Depinho, R. A. *Nat. Rev. Mol. Cell Biol.* **2007**, *8*, 703–713.
(7) Brandon, M.; Baldi, P.; Wallace, D. C. *Oncogene* **2006**, *25*, 4647–4662.
(8) Finkel, T.; Serrano, M.; Blasco, M. A. *Nature* **2007**, *448*, 767–774.
(9) Fruehauf, J. P.; Meyskens, F. L. *Clin. Cancer Res.* **2007**, *13*, 789–794.
(10) Ishikawa, K.; Takenaga, K.; Akimoto, M.; Koshikawa, N.; Yamaguchi, A.; Imanishi, H.; Nakada, K.; Honma, Y.; Hayashi, J. *Science* **2008**, *320*, 661–664.
(11) Goetz, M. E.; Luch, A. *Cancer Lett.* **2008**, *266*, 73–83.
(12) Rossi, D. J.; Jamieson, C. H. M.; Weissman, I. L. *Cell* **2008**, *132*, 681–696.
(13) Houstis, N.; Rosen, E. D.; Lander, E. S. *Nature* **2006**, *440*, 944–948.
(14) Jay, D.; Hitomi, H.; Griendling, K. K. *Free Radical Biol. Med.* **2006**, *40*, 183–192.
(15) Pop-Busui, R.; Sima, A.; Stevens, M. *Diabetes-Metab. Res. Rev.* **2006**, *22*, 257–273.
(16) Barnham, K. J.; Masters, C. L.; Bush, A. I. *Nat. Rev. Drug Discov.* **2004**, *3*, 205–214.
(17) Lin, M. T.; Beal, M. F. *Nature* **2006**, *443*, 787–795.
(18) DiMauro, S.; Schon, E. A. *Annu. Rev. Neurosci.* **2008**, *31*, 91–123.
(19) Rhee, S. G. *Science* **2006**, *312*, 1882–1883.
(20) Stone, J. R.; Yang, S. *Antioxid. Redox Signal.* **2006**, *8*, 243–270.
(21) D'AutrEaux, B.; Toledano, M. B. *Nat. Rev. Mol. Cell Biol.* **2007**, *8*, 813–824.
(22) Giorgio, M.; Trinei, M.; Migliaccio, E.; Pelicci, P. G. *Nat. Rev. Mol. Cell Biol.* **2007**, *8*, 722–728.
(23) Valko, M.; Leibfritz, D.; Moncol, J.; Cronin, M. T. D.; Mazur, M.; Telser, J. *Int. J. Biochem. Cell Biol.* **2007**, *39*, 44–84.
(24) Miller, E. W.; Chang, C. J. *Curr. Opin. Chem. Biol.* **2007**, *11*, 620–625.
(25) Veal, E. A.; Day, A. M.; Morgan, B. A. *Mol. Cell* **2007**, *26*, 1–14.
(26) Winterbourn, C. C. *Nat. Chem. Biol.* **2008**, *4*, 278–286.
(27) Segal, A. W.; Abo, A. *Trends Biochem. Sci.* **1993**, *18*, 43–47.
(28) Lambeth, J. D. *Nat. Rev. Immunol.* **2004**, *4*, 181–189.
(29) Bedard, K.; Krause, K. H. *Physiol. Rev.* **2007**, *87*, 245–313.

participant in oxidative stress and damage. Whereas high concentrations of H_2O_2 can trigger apoptotic or necrotic cell death, controlled bursts of H_2O_2 produced in response to stimulation by various growth factors, cytokines, and neurotransmitters can act as secondary messengers to signal cell growth, proliferation, and differentiation.[19−26,30−39]

Because variations in the spatial and temporal production of H_2O_2 lead to disparate downstream biological effects, new methods that allow detection of this ROS in living systems with subcellular resolution can help decipher its complex cellular chemistry. To this end, an elegant example of a fluorescent protein sensor based on a circularly permuted YFP with an OxyR insert has been reported for cellular H_2O_2 detection.[40] We envisioned developing an alternative chemical biology approach that combines the versatility of small-molecule reporters with the targetability of genetically encodable protein scaffolds for subcellular localization. Currently, selective protein labeling in living cells with synthetic compounds is feasible in either a covalent or noncovalent manner.[41−45] Noncovalent labeling methods utilizing the specific binding of ligands to short peptide or protein domains include the binding of biarsenic compounds to tetracysteine haiprins (FlAsH, ReAsH),[46] the binding of a metal complex to oligo-His[47,48] or oligo-Asp motifs,[49] the recognition of trimethoprim by dihydrofolate reductase,[50,51] and a high affinity binding interaction of protein FKBP12(F36 V) with its ligand FK-SLF.[52] Examples of covalent self-labeling mediated by fusion enzymes include attachment of alkyl chlorides to dehalogenase enzymes (HaloTag),[53−55] formation of covalent adduct between cutinase and *p*-nitrophenyl phosphonate (pNPP) derivatives,[56] labeling of AGT (O^6-alkyguanine-DNA alkyltransferase) fusion proteins with SNAP/CLIP substrates,[57−59] and covalent labeling by enzymes involved in post-translation modifications such as phosphopantetheine transferase,[60,61] transglutaminase,[62,63] biotin ligase BirA,[64,65] lipoic acid ligase,[66] sortaseA,[67,68] protein farnesyltransferase,[69] and formylglycine generating enzyme.[70,71] In particular, we were attracted to the SNAP tag technology, which within a short time after its invention by Johnsson and co-workers, has found broad utility in a variety of biological applications. Use of the SNAP tag allows precise targeting of bioactive reagents or probes to specific subcellular locales; recent examples include photosensitizers for chomophore-assisted laser inactivation (CALI) of fusion proteins[72] and fluorescent sensors for intracellular metal ions including zinc(II)[73] and calcium(II).[74] Simultaneous labeling of two different targets can also be achieved using tandem SNAP and CLIP tags.[59] The SNAP tag has been used for protein tracking with spatial and temporal resolution, where a fusion protein at a given time point is initially marked by a fluorescent or nonfluorescent SNAP tag substrate label, and subsequent newly synthesized proteins can be differentiated by a second label.[59,75] Other applications of the SNAP tag technology include its use in combination with fluorescent proteins as FRET-based reporters for studying

(30) Sundaresan, M.; Yu, Z. X.; Ferrans, V. J.; Irani, K.; Finkel, T. *Science* **1995**, *270*, 296–299.
(31) Bae, Y. S.; Kang, S. W.; Seo, M. S.; Baines, I. C.; Tekle, E.; Chock, P. B.; Rhee, S. G. *J. Biol. Chem.* **1997**, *272*, 217–221.
(32) Avshalumov, M. V.; Chen, B. T.; Marshall, S. P.; Pena, D. M.; Rice, M. E. *J. Neurosci.* **2003**, *23*, 2744–2750.
(33) Tonks, N. K. *Cell* **2005**, *121*, 667–670.
(34) Poole, L. B.; Nelson, K. J. *Curr. Opin. Chem. Biol.* **2008**, *12*, 18–24.
(35) Bao, L.; Avshalumov, M. V.; Patel, J. C.; Lee, C. R.; Miller, E. W.; Chang, C. J.; Rice, M. E. *J. Neurosci.* **2009**, *29*, 9002–9010.
(36) Eligini, S.; Arenaz, I.; Barbieri, S. S.; Faleri, M. L.; Crisci, M.; Tremoli, E.; Colli, S. *Free Radical Biol. Med.* **2009**, *46*, 1428–1436.
(37) Kim, J. S.; Huang, T. Y.; Bokoch, G. M. *Mol. Biol. Cell* **2009**, *20*, 2650–2660.
(38) Leonard, S. E.; Reddie, K. G.; Carroll, K. S. *ACS Chem. Biol.* **2009**, *4*, 783–799.
(39) Niethammer, P.; Grabher, C.; Look, A. T.; Mitchison, T. J. *Nature* **2009**, *459*, 996–999.
(40) Belousov, V. V.; Fradkov, A. F.; Lukyanov, K. A.; Staroverov, D. B.; Shakhbazov, K. S.; Terskikh, A. V.; Lukyanov, S. *Nat. Methods* **2006**, *3*, 281–286.
(41) Chen, I.; Ting, A. Y. *Curr. Opin. Biotechnol.* **2005**, *16*, 35–40.
(42) Gronemeyer, T.; Godin, G.; Johnsson, K. *Curr. Opin. Biotechnol.* **2005**, *16*, 453–458.
(43) Miller, L. W.; Cornish, V. W. *Curr. Opin. Chem. Biol.* **2005**, *9*, 56–61.
(44) Chattopadhaya, S.; Abu Bakar, F. B.; Yao, S. Q. *Curr. Med. Chem.* **2009**, *16*, 4527–4543.
(45) Sletten, E. M.; Bertozzi, C. R. *Angew. Chem., Int. Ed.* **2009**, *48*, 6974–6998.
(46) Griffin, B. A.; Adams, S. R.; Tsien, R. Y. *Science* **1998**, *281*, 269–272.
(47) Guignet, E. G.; Hovius, R.; Vogel, H. *Nat. Biotechnol.* **2004**, *22*, 440–444.
(48) Hauser, C. T.; Tsien, R. Y. *Proc. Natl. Acad. Sci. U.S.A.* **2007**, *104*, 3693–3697.
(49) Ojida, A.; Honda, K.; Shinmi, D.; Kiyonaka, S.; Mori, Y.; Hamachi, I. *J. Am. Chem. Soc.* **2006**, *128*, 10452–10459.
(50) Calloway, N. T.; Choob, M.; Sanz, A.; Sheetz, M. P.; Miller, L. W.; Cornish, V. W. *ChemBioChem* **2007**, *8*, 767–774.
(51) Gallagher, S. S.; Sable, J. E.; Sheetz, M. P.; Cornish, V. W. *ACS Chem. Biol.* **2009**, *4*, 547–556.
(52) Marks, K. M.; Braun, P. D.; Nolan, G. P. *Proc. Natl. Acad. Sci. U. S. A.* **2004**, *101*, 9982–9987.
(53) Zhang, Y.; So, M. K.; Loening, A. M.; Yao, H. Q.; Gambhir, S. S.; Rao, J. H. *Angew. Chem., Int. Ed.* **2006**, *45*, 4936–4940.
(54) Los, G. V.; et al. *ACS Chem. Biol.* **2008**, *3*, 373–382.
(55) Watkins, R. W.; Lavis, L. D.; Kung, V. M.; Los, G. V.; Raines, R. T. *Org. Biomol. Chem.* **2009**, *7*, 3969–3975.
(56) Bonasio, R.; Carman, C. V.; Kim, E.; Sage, P. T.; Love, K. R.; Mempel, T. R.; Springer, T. A.; von Andrian, U. H. *Proc. Natl. Acad. Sci. U.S.A.* **2007**, *104*, 14753–14758.
(57) Juillerat, A.; Gronemeyer, T.; Keppler, A.; Gendreizig, S.; Pick, H.; Vogel, H.; Johnsson, K. *Chem. Biol.* **2003**, *10*, 313–317.
(58) Keppler, A.; Kindermann, M.; Gendreizig, S.; Pick, H.; Vogel, H.; Johnsson, K. *Methods* **2004**, *32*, 437–444.
(59) Gautier, A.; Juillerat, A.; Heinis, C.; Correa, I. R.; Kindermann, M.; Beaufils, F.; Johnsson, K. *Chem. Biol.* **2008**, *15*, 128–136.
(60) Yin, J.; Straight, P. D.; McLoughlin, S. M.; Zhou, Z.; Lin, A. J.; Golan, D. E.; Kelleher, N. L.; Kolter, R.; Walsh, C. T. *Proc. Natl. Acad. Sci. U.S.A.* **2005**, *102*, 15815–15820.
(61) Zhou, Z.; Cironi, P.; Lin, A. J.; Xu, Y. Q.; Hrvatin, S.; Golan, D. E.; Silver, P. A.; Walsh, C. T.; Yin, J. *ACS Chem. Biol.* **2007**, *2*, 337–346.
(62) Lorand, L.; Graham, R. M. *Nat. Rev. Mol. Cell Biol.* **2003**, *4*, 140–156.
(63) Lin, C. W.; Ting, A. Y. *J. Am. Chem. Soc.* **2006**, *128*, 4542–4543.
(64) Chen, I.; Howarth, M.; Lin, W. Y.; Ting, A. Y. *Nat. Methods* **2005**, *2*, 99–104.
(65) Howarth, M.; Takao, K.; Hayashi, Y.; Ting, A. Y. *Proc. Natl. Acad. Sci. U.S.A.* **2005**, *102*, 7583–7588.
(66) Fernandez-Suarez, M.; Baruah, H.; Martinez-Hernandez, L.; Xie, K. T.; Baskin, J. M.; Bertozzi, C. R.; Ting, A. Y. *Nat. Biotechnol.* **2007**, *25*, 1483–1487.
(67) Popp, M. W.; Antos, J. M.; Grotenbreg, G. M.; Spooner, E.; Ploegh, H. L. *Nat. Chem. Biol.* **2007**, *3*, 707–708.
(68) Tanaka, T.; Yamamoto, T.; Tsukiji, S.; Nagamune, T. *ChemBioChem* **2008**, *9*, 802–807.
(69) Duckworth, B. P.; Zhang, Z. Y.; Hosokawa, A.; Distefano, M. D. *ChemBioChem* **2007**, *8*, 98–105.
(70) Carrico, I. S.; Carlson, B. L.; Bertozzi, C. R. *Nat. Chem. Biol.* **2007**, *3*, 321–322.
(71) Wu, P.; Shui, W. Q.; Carlson, B. L.; Hu, N.; Rabuka, D.; Lee, J.; Bertozzi, C. R. *Proc. Nat. Acad. Sci. U. S. A.* **2009**, *106*, 3000–3005.
(72) Keppler, A.; Ellenberg, J. *ACS Chem. Biol.* **2009**, *4*, 127–138.
(73) Tomat, E.; Nolan, E. M.; Jaworski, J.; Lippard, S. J. *J. Am. Chem. Soc.* **2008**, *130*, 15776–15777.
(74) Bannwarth, M.; Correa, I. R.; Sztretye, M.; Pouvreau, S.; Fellay, C.; Aebischer, A.; Royer, L.; Rios, E.; Johnsson, K. *ACS Chem. Biol.* **2009**, *4*, 179–190.
(75) Farr, G. A.; Hull, M.; Mellman, I.; Caplan, M. J. *J. Cell. Biol.* **2009**, *186*, 269–282.

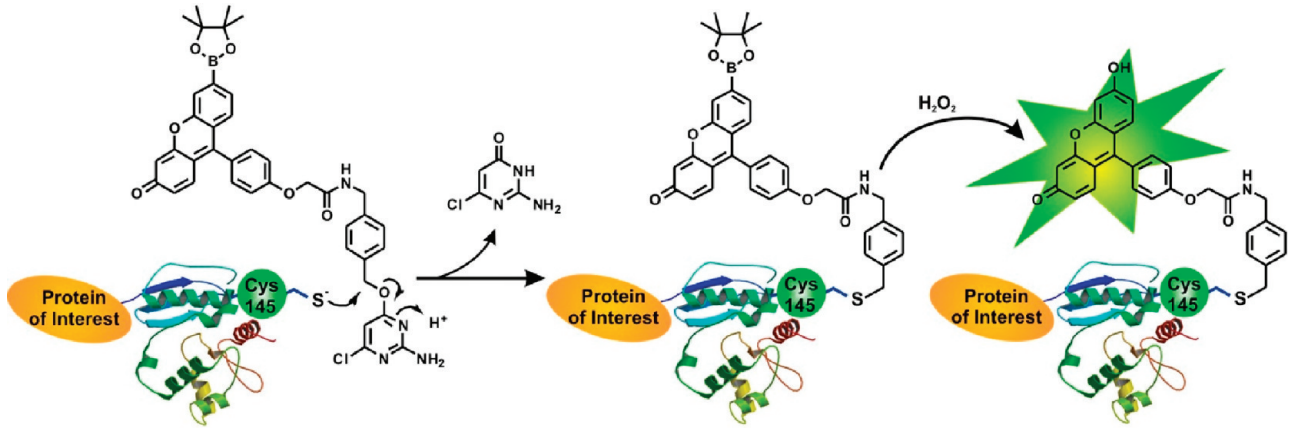

Figure 1. Design strategy for organelle-specific hydrogen peroxide reporters using the SNAP tag methodology.

protein−protein interactions[76] and the development of semisynthetic fluorescent sensors or photoactivable switches.[77,78]

In this report, we present the design, synthesis, properties, and cellular applications of a new class of organelle-targetable fluorescent probes for H_2O_2 based on SNAP-AGT bioconjugation chemistry. We have prepared and characterized a pair of boronate-caged, Peroxy Green-type fluorescent peroxide indicators bearing the SNAP substrates, where one is a membrane-permeable version for intracellular use and another is a membrane-impermeable version for cell surface labeling, and coupled them to AGT proteins expressed in various cellular compartments. The resulting SNAP-Peroxy Green (SNAP-PG) hybrid small-molecule/protein conjugates are capable of detecting H_2O_2 over a variety of ROS and can be targeted to various subcellular locales, including the plasma membrane, nucleus, mitochondrial inner membrane, and endoplasmic reticulum, to sense changes in H_2O_2 levels within or on the surface of living cells. This method provides a general platform for studying the chemistry of H_2O_2 by molecular imaging in living biological specimens with subcellular resolution.

Results and Discussion

Design and Synthesis of SNAP-Peroxy-Green Bioconjugates as Organelle-Targetable Fluorescent Reporters for Cellular Hydrogen Peroxide. Figure 1 depicts our overall strategy for creating subcellular-targetable fluorescent H_2O_2 probes by combining the SNAP-tag methodology for site-specific labeling[79,80] with the chemoselective H_2O_2-mediated deprotection of boronate esters to phenols for reaction-based detection of H_2O_2.[81−86] Fusion of AGT with proteins containing a signaling sequence allows expression of AGT in defined subcellular compartments. These localized AGT scaffolds can then be tagged by covalent labeling at Cys145 with a boronate PG fluorescent probe bearing an appended SNAP substrate. The resulting SNAP-PG conjugates are hybrid small-molecule/protein reporters that give a fluorescent turn-on response upon H_2O_2-mediated boronate cleavage.

Scheme 1. Synthesis of SNAP-Tag Substrates

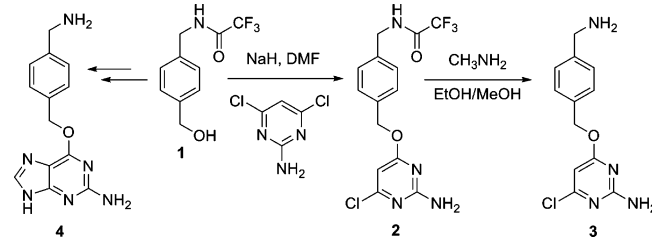

To this end, we previously reported the synthesis and application of Peroxy Green 1 (PG1),[87] a cell-permeable and selective H_2O_2 probe that can be activated by a single boronate deprotection. Along these lines, we sought to create PG1 analogs for organelle-specific labeling by replacing its 4-methoxy moiety with benzylguanine or benzyl-2-chloro-6-aminopyrimidine SNAP tag substrates. Scheme 1 depicts the synthesis of SNAP tag derivatives for coupling to a PG1 scaffold. Benzylguanine **4** was synthesized according to literature protocols.[58] In a similar manner, benzyl-2-chloro-6-aminopyrimide **3** was synthesized by nucleophilic substitution of 2,6-dichloropyrimidin-4-amine with trifluoro-*N*-(4-hydroxymethyl-benzyl)-acetamide **1**. The trifluoroacetamide protecting group was subsequently removed with 33% methylamine in ethanol.

Scheme 2 details the synthesis of SNAP-Peroxy Green-1 (SPG1) and SNAP-Peroxy Green-2 (SPG2) probes by coupling the aforementioned SNAP tag substrates with a carboxylate-derivatized PG1; the latter is prepared in five steps from the fluorescein-like dye Tokyo Green (TG).[88] Treatment of TG **5** with boron tribromide at −78 °C in dry CH_2Cl_2 furnishes the phenolic TG **6**. *O*-alkylation of **6** in anhydrous DMF with excess

(76) Maurel, D.; Comps-Agrar, L.; Brock, C.; Rives, M. L.; Bourrier, E.; Ayoub, M. A.; Bazin, H.; Tinel, N.; Durroux, T.; Prezeau, L.; Trinquet, E.; Pin, J. P. *Nat. Methods* **2008**, *5*, 561–567.
(77) Mao, S.; Benninger, R. K. P.; Yan, Y. L.; Petchprayoon, C.; Jackson, D.; Easley, C. J.; Piston, D. W.; Marriott, G. *Biophys. J.* **2008**, *94*, 4515–4524.
(78) Brun, M. A.; Tan, K. T.; Nakata, E.; Hinner, M. J.; Johnsson, K. *J. Am. Chem. Soc.* **2009**, *131*, 5873–5884.
(79) Keppler, A.; Gendreizig, S.; Gronemeyer, T.; Pick, H.; Vogel, H.; Johnsson, K. *Nat. Biotechnol.* **2003**, *21*, 86–89.
(80) Keppler, A.; Pick, H.; Arrivoli, C.; Vogel, H.; Johnsson, K. *Proc. Nat. Acad. Sci. U. S. A.* **2004**, *101*, 9955–9959.
(81) Chang, M. C. Y.; Pralle, A.; Isacoff, E. Y.; Chang, C. J. *J. Am. Chem. Soc.* **2004**, *126*, 15392–15393.
(82) Miller, E. W.; Albers, A. E.; Pralle, A.; Isacoff, E. Y.; Chang, C. J. *J. Am. Chem. Soc.* **2005**, *127*, 16652–16659.
(83) Albers, A. E.; Okreglak, V. S.; Chang, C. J. *J. Am. Chem. Soc.* **2006**, *128*, 9640–9641.
(84) Albers, A. E.; Dickinson, B. C.; Miller, E. W.; Chang, C. J. *Bioorg. Med. Chem. Lett.* **2008**, *18*, 5948–5950.
(85) Srikun, D.; Miller, E. W.; Domaille, D. W.; Chang, C. J. *J. Am. Chem. Soc.* **2008**, *130*, 4596–4597.
(86) Dickinson, B. C.; Chang, C. J. *J. Am. Chem. Soc.* **2008**, *130*, 11561–11562.
(87) Miller, E. W.; Tulyathan, O.; Isacoff, E. Y.; Chang, C. J. *Nat. Chem. Biol.* **2007**, *3*, 263–267.
(88) Urano, Y.; Kamiya, M.; Kanda, K.; Ueno, T.; Hirose, K.; Nagano, T. *J. Am. Chem. Soc.* **2005**, *127*, 4888–4894.

Scheme 2. Synthesis of SPG1 and SPG2

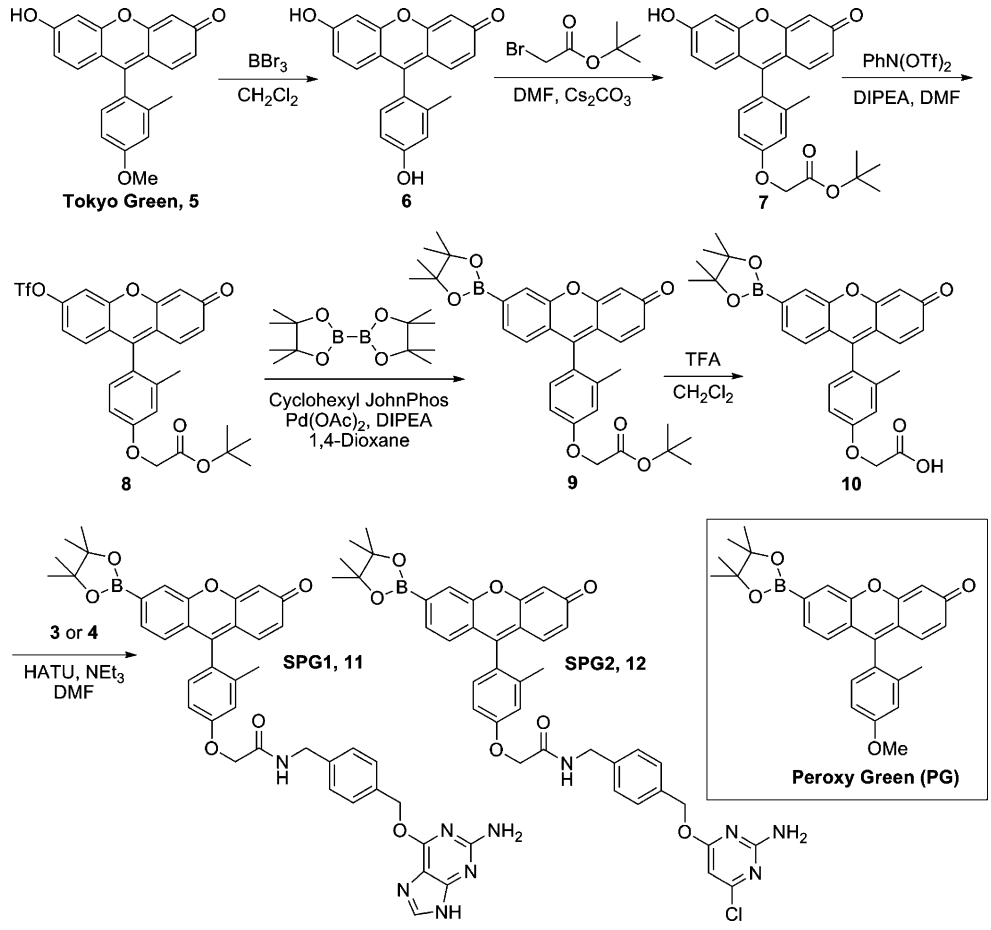

Scheme 3. Synthesis of STG1 and STG2

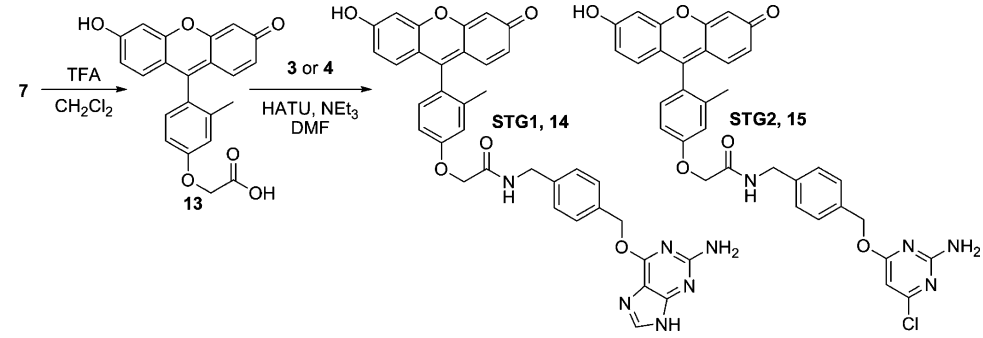

cesium carbonate and a slow addition of *tert*-butylbromoacetate gives *tert*-butyl ester TG **7**. Reaction of **7** with bis(trifluoromethane)sulfonamide affords triflate **8**. Palladium-mediated borylation of triflate **8** with bis(pinacolato)diboron, cyclohexyl JohnPhos, and diisopropylethylamine in anhydrous 1,4-dioxane provides boronic ester **9**. Subsequent treatment with trifluoroacetic acid in anhydrous CH_2Cl_2 delivers carboxylate PG **10**. Amide bond formation between the carboxyl PG **10** and the SNAP substrate **4** or **3** mediated by *N,N,N′,N′*-tetramethyl-*O*-(7-azabenzotriazol-1-yl)uroniumhexafluorophosphate (HATU) affords SPG1 (**11**) or SPG2 (**12**), respectively.

Finally, we also synthesized TG analogs bearing SNAP tags **3** or **4** as control compounds for cell labeling and imaging as shown in Scheme 3. Treatment of *tert*-butyl ester TG **7** with TFA furnishes carboxyl TG **13**. The HATU-mediated amide coupling of **13** with either **4** or **3** provides SNAP-TG-1 (STG1, **14**) and SNAP-TG-2 (STG2, **15**), respectively.

Spectroscopic Properties, In Vitro Protein AGT Labeling, and Peroxide Responses of SNAP-PG and SNAP-TG Fluorophores. Table 1 summarizes the spectroscopic properties of the SNAP-PG and SNAP-TG fluorophores in aqueous buffer at neutral pH (20 mM HEPES, pH 7). SPG1 and SPG2 both show visible absorption bands centered at 465 nm (SPG1: $\varepsilon = 10\,200$ M^{-1} cm^{-1}, SPG2: $\varepsilon = 9800$ M^{-1} cm^{-1}) and weak fluorescence with an emission maximum at 515 nm. In contrast, the STG1 and STG2 fluorophores exhibit a prominent absorption at 495 nm (STG1: $\varepsilon = 36\,000$ M^{-1} cm^{-1}, STG2: $\varepsilon = 37\,000$ M^{-1} cm^{-1}) and fluorescent emission maximum at 513 nm. The quantum yield of STG1 ($\Phi = 0.12$) is much lower than that of STG2 ($\Phi = 0.87$), presumably due to the greater quenching

Table 1. Spectroscopic Properties of SNAP Dyes and Their AGT Bioconjugates

compound	λ_{exc} (nm)	(M^{-1} cm^{-1})	λ_{em} (nm)	Φ
STG1	495	36000	513	0.12
STG2	495	37000	513	0.87
AGT-TG	500	32000	515	0.57
SPG1	465	10200	515	0.10
SPG2	465	9800	515	0.09
AGT-PG	465	11500	515	0.07

effect of guanidine moiety; a similar effect has been observed in other SNAP fluorophores.[73] We thus proceeded to test the H_2O_2 reactivity of these free dyes with the SPG2 analog. Reaction of SPG2 with 1 mM H_2O_2 triggers a ca. 32-fold fluorescence turn-on for the dye (Figure S11) confirming the peroxide response of these SNAP tag reporters. Kinetics measurements of the SPG2 boronate deprotection performed under pseudo-first-order conditions (1 μM dye, 1 mM H_2O_2) give an observed rate constant of $k_{obs} = 1.0(1) \times 10^{-3}$ s^{-1}.

We next proceeded to test the ability of the SPG and STG dyes to label purified AGT protein samples and to evaluate the spectroscopic properties and peroxide responses of the isolated fluorophore-protein conjugates. For these in vitro protein labeling assays, hexahistidine-tagged AGT (His-AGT) was overexpressed in *E. coli* and purified with a standard Ni-NTA affinity column. After incubation of His-tagged AGT with SPG1, SPG2, STG1, or STG2 dyes in 20 mM HEPES at pH 7 for 30 min at 37 °C, we confirmed the formation of the desired covalently labeled products, AGT-PG and AGT-TG, by both LC-MS and 488 nm excitation in-gel fluorescence measurements (Supporting Information, Figures S1 to S7). Specifically, AGT-TG and AGT-PG show mass increases of 478 and 506 Da, respectively, from His-tagged AGT; these values are consistent with the calculated mass of the protein tagged with TG or the boronic acid form of PG, respectively. We purified the AGT-PG and AGT-TG bioconjugates for further spectroscopic evaluation using MWCO spin columns and size-exclusive gel chromatography to remove the free organic fluorophores. This dual purification method is essential to obtain clean dye−protein conjugates without interference from small-molecule impurities. In addition, the labeling proceeds well under oxidizing conditions, as we observe covalent adduct formation in the presence up to 1 mM H_2O_2 (Figure S2). AGT-TG possesses a dominant absorption maximum in the visible region centered at 500 nm, which is slightly red-shifted relative the free TG dye. The AGT-TG complex shows prominent absorption at 280 (standard protein absorption) and 500 nm (TG dye), consistent with labeling of the AGT protein with the small-molecule TG payload (Figure S8). Furthermore, formation of AGT-TG conjugate is also reflected in the observed fluorescence quantum yield, as binding of STG1 to AGT ejects guanidine from the dye and eliminates its quenching effect, resulting in a 6-fold fluorescence increase (Figure S9). The absorption and emission spectra of AGT-PG are similar to SPG1 and SPG2, with an additional 280 nm absorption due to the AGT protein.

Importantly, the SPG dyes are able to retain their fluorescence response to H_2O_2 upon protein labeling, as purified AGT-PG conjugates exhibit a marked turn-on emission response to added H_2O_2 (Figure 2). The H_2O_2-induced fluorescence increases occur with concomitant growth of the characteristic TG absorption at 500 nm, consistent with boronate cleavage of PG to produce the phenol TG product (Figure 3). Finally, we observe a linear correlation between various H_2O_2 concentrations added and observed fluorescence emission responses (Figure 4).

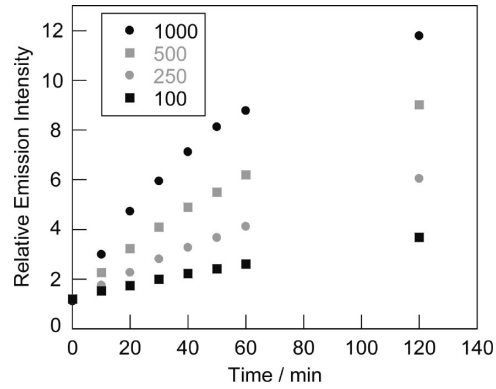

Figure 2. Fluorescence responses of 1 μM AGT-PG, a conjugate formed from the reaction of AGT with SPG2, to 100, 250, 500, and 1000 μM H_2O_2 in 20 mM HEPES, pH 7 at 25 °C. The plot shows emission responses at 0, 10, 20, 30, 40, 50, 60, and 120 min after H_2O_2 addition. The reactions are not complete at these early time points. The collected emission was integrated between 500−650 nm (λ_{exc} = 488 nm).

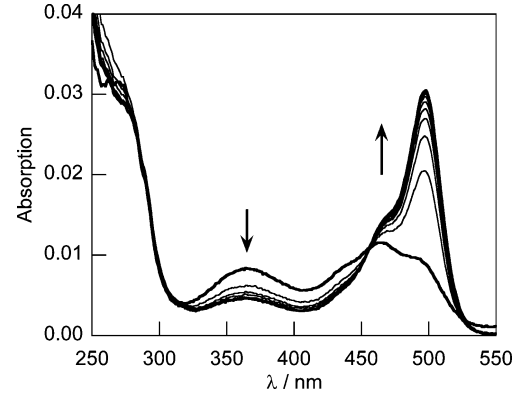

Figure 3. Absorption spectra of 1 μM AGT-PG in 20 mM HEPES, pH 7 upon addition of 1 mM H_2O_2. Spectra were acquired at 1 h intervals for 8 h. An isosbestic point was observed at 460 nm.

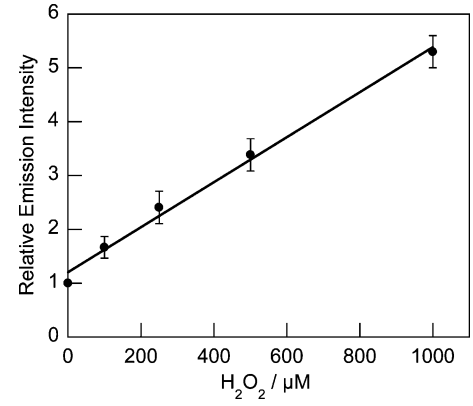

Figure 4. Fluorescence responses of 1 μM AGT-PG to various concentrations of added H_2O_2. Spectra were acquired in 20 mM HEPES, pH 7 at 25 °C after incubation of the probe with H_2O_2 for 30 min. Reactions are not complete at this early time point. The collected emission was integrated between 500−650 nm (λ_{exc} = 488 nm). Error bars represent standard deviation.

Fluorescence Detection of H_2O_2 in Various Compartments of Living Cells with SNAP-AGT PG Reporters. With spectroscopic data establishing the formation of AGT-PG conjugates and their fluorescence turn-on response to H_2O_2, we next sought to apply SPG1 and SPG2 for optical detection of H_2O_2 in living biological samples. Specifically, we focused on directing these

probes to a broad range of subcellular compartments that are either capable of locally generating H_2O_2 in response to various stimuli or to sites where their function and regulation are sensitive to H_2O_2 flux. In this study, we targeted SPG reporters to a broad spectrum of locations. Included are the plasma membrane, mitochondria, endoplasmic reticulum, and nucleus. To this end, plasmids for expression of the SNAP-tag in live mammalian cells were obtained from Covalys and then subjected to further modification as necessary. The parent SNAP-tag without a signaling sequence (pSNAP), encoding a genetically optimized AGT protein, gives a uniform intracellular expression of SNAP-tag in the cytoplasm and the nucleus. Localization of the SNAP-tag to nucleus is achieved by fusion of SNAP-tag to the C-terminus of the histone H2B protein (SNAP-H2B). Fusion of the SNAP-tag to the C-terminus of cytochrome *c* oxidase subunit 8 (Cox8A) enables its localization to the mitochondrial inner membrane (SNAP-Cox8A). For plasma membrane targeting, the SNAP-tag is expressed as a fusion to the N-terminus of neurokinin-1 receptor (NK1R) and the C-terminus of 5HT3A serotonin receptor signaling sequence, resulting in a SNAP-tag exposed to the extracellular space (SNAP-NK1R). Addition of KDEL, a signaling peptide for retention of the protein in endoplasmic reticulum (ER), to the C-terminus of SNAP results in an ER localized SNAP-tag (SNAP-KDEL).

We first tested the site-specific labeling of various SNAP fusion proteins with control STG1 and STG2 dyes in live HEK293T cells. To our surprise, we found that STG1 and STG2 exhibit marked differences in cell permeability that can be exploited to obtain more selective conjugation to extracellular and intracellular spaces. Specifically, whereas both STG1 and STG2 gave excellent membrane labeling with SNAP-NK1R, intracellular tagging of pSNAP and SNAP-H2B was observed only with STG2 (Figure 5). The same trend applies to SPG1 and SPG2, where only the latter is membrane permeable. Our findings are consistent with previous work that reports that benzylguanine can hamper the cell permeability of its conjugated partners in a fluorophore-dependent manner.[58,89] STG2 shows desirable properties for intracellular site-specific labeling applications, as the dye is cell permeable and the unbound probe can be readily washed out. This latter property is crucial to minimizing background fluorescence from nonspecific or off-target labeling. Indeed, in HEK293T cells transiently expressing SNAP-KDEL and SNAP-Cox8A to target the endoplasmic reticulum and mitochondria, respectively, we were able to successfully tag these organelles with STG2. The subcellular localization of this dye to these compartments was confirmed by fluorescence overlay of green emissive STG2 with red emission from mCherry-KDEL and mCherry-Cox8A constructs (Figure 6).

Recognizing these SNAP-tag-dependent differences in membrane permeability, we then proceeded to evaluate the boronate SPG1 and SPG2 reporters for site-specific subcellular H_2O_2 detection, employing SPG1 for extracellular plasma membrane targeting and SPG2 for intracellular labeling. We utilized real-time imaging of the same cells before and after oxidative stimulation or in untreated samples. This method allows us to perform an important control for varying levels of protein expression as well as a control to show that photodynamic oxidation is not significant with these systems. For extracellular measurements, HEK293T cells transiently expressing SNAP-

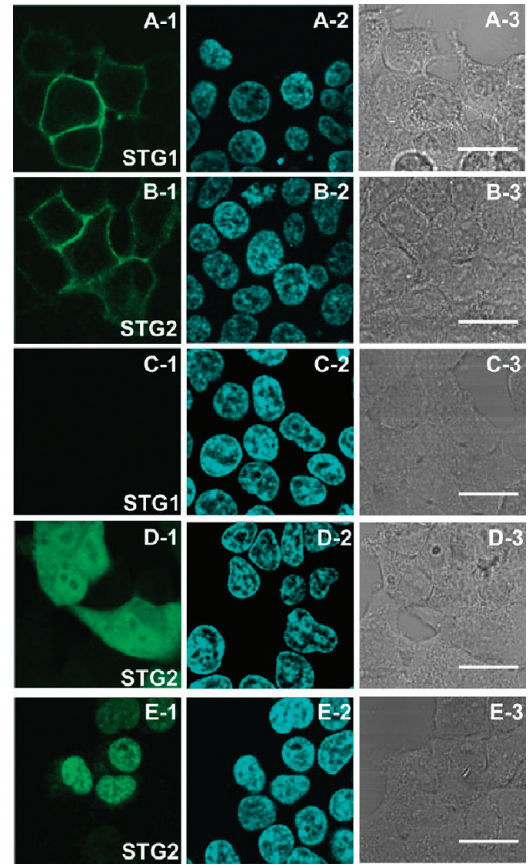

Figure 5. Targeted localization of STG1 and STG2 in living HEK293T cells by conjugation to SNAP-AGT fusion proteins. Cells were incubated with 5 μM STG1 or STG2 for 30 min, and washed with fresh DMEM + 10% FBS for 30 min (2 × 1 mL) before image acquisition. Rows (A) and (B) show HEK 293T cells transiently expressing SNAP-NK1R. Rows (C) and (D) display HEK 293T cells transiently expressing pSNAP for nonspecific intracellular tagging, and row (E) presents HEK 293T cells transiently expressing SNAP-H2B. For each series: (1) emission from labeling with STG1 or STG2, (2) nuclear staining with Hoechst 33342, and (3) brightfield image. Scale bar = 20 μm.

NK1R display weak but detectable green fluorescent emission localized to the plasma membrane after SPG1 conjugation. The relatively poor membrane permeability of this probe allows for rapid and selective labeling of cell surfaces with washing. Treatment of SPG1-labeled cells with 100 μM H_2O_2 triggers a marked increase in fluorescence from the plasma membrane region as shown by time lapse image acquisitions (Figure 7a). Importantly, negligible emission comes from nontransfected cells in the same image frame even after treatment with H_2O_2, establishing that specific SPG1 binding to the SNAP-NK1R fusion protein scaffold is required for imaging changes in H_2O_2 levels localized to the plasma membrane. As a further control, we do not observe fluorescence turn-on responses for SPG1-loaded cells in the absence of H_2O_2, and a combination of nuclear staining and brightfield transmission measurements confirm that the cells are viable throughout the imaging experiments.

To label intracellular compartments, we subjected cells to 5 μM SPG2 for 30 min followed by a 30 min incubation in fresh complete medium (DMEM + 10% FBS) to wash out any unbound probe. HEK293T cells transiently expressing pSNAP display weak intracellular fluorescent emission after labeling with SPG2. Addition of 100 μM H_2O_2 to the cells results in a patent increase in overall intracellular fluorescence from this

(89) Keppler, A.; Arrivoli, C.; Sironi, L.; Ellenberg, J. *Biotechniques* **2006**, *41*, 167–175.

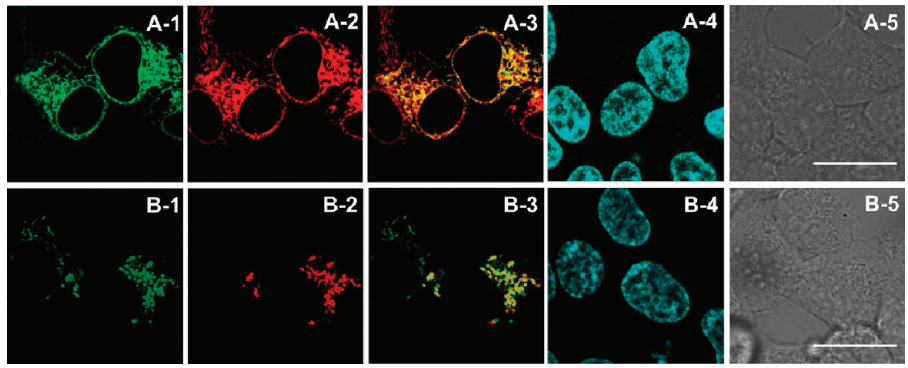

Figure 6. Targeted labeling of endoplasmic reticulum and mitochondria organelles with STG2. Row (A) shows HEK 293T cells expressing SNAP-KDEL in the ER lumen, and row (B) depicts HEK 293T cells expressing SNAP-Cox8A for mitochondrial tagging. For each series: (1) emission from labeling with STG2, (2) emission from (a) mCherry-KDEL or (b) mCherry-Cox8A, (3) overlay of STG2 and mCherrry, (4) nuclear staining with Hoechst 33342, and (5) brightfield image. Scale bar = 20 μm.

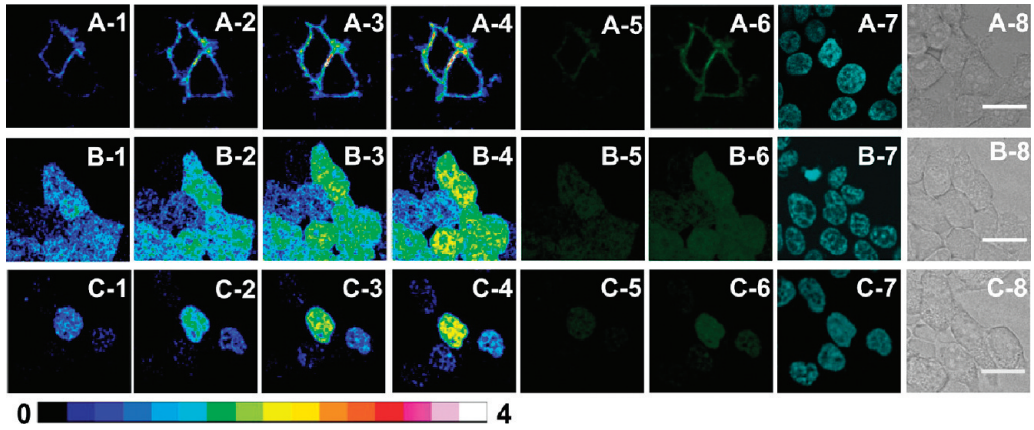

Figure 7. Fluorescence detection of H_2O_2 on the surface of or within living HEK 293T cells. Row (A) shows cells transiently expressing SNAP-NK1R tagged with SPG1, row (B) displays cells transiently expressing pSNAP tagged with SPG2, and row (C) presents cells transiently expressing SNAP-H2B tagged with SPG2. H_2O_2 was added from 50 mM solution in Mili-Q water. Time-lapse image acquisition was assisted by a motorized stage equipped with incubator and humidifier maintaining 37 °C and 5% CO_2 atmosphere. For each series: (1−4) pseudocolor mode of fluorescent emission at 0, 10, 20, and 30 min after addition of 100 μM H_2O_2, (5, 6) fluorescent emission before (5) and after (6) treatment of cells with 100 μM H_2O_2 for 30 min (λ_{exc} = 488 nm, λ_{em} = 500−550 nm), (7) nuclear staining with Hoechst 33342, (8) brightfield image. Scale bar = 20 μm.

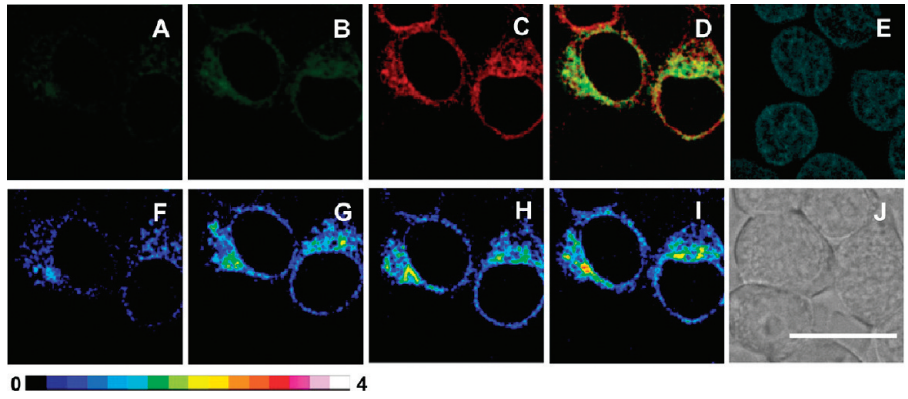

Figure 8. Fluorescence detection of H_2O_2 in living HEK 293T cells transiently expressing SNAP-KDEL and mCherry-KDEL. Panels (A) and (B) show fluorescent emission from cells labeled with SPG2 before (A) and after (B) treatment with 100 μM H_2O_2 for 30 min (λ_{exc} = 488 nm, λ_{em} = 500−550 nm), panel (C) presents emission from mCherry-KDEL, panel (D) displays the overlay of (B) and (C), panel (E) shows nuclear staining with Hoechst 33342, and panels (F−I) display pseudocolor fluorescent emission at 0, 10, 20, and 30 min after addition of 100 μM H_2O_2. Panel (J) presents the brightfield image of cells in (I). Scale bar = 20 μm.

protein/small-molecule reporter (Figure 7b). Likewise, SPG2-loaded HEK293T cells transiently expressing SNAP-H2B show nuclear-localized fluorescence that becomes more intense after stimulation with H_2O_2 (Figure 7c). Moreover, SPG2 can be precisely immobilized onto the mitochondrial inner membrane and ER regions of HEK293T cells transiently expressing SNAP-Cox8A (Figure 8) and SNAP-KDEL (Figure 9), respectively. In both cases, the turn-on green fluorescence emission from the SNAP-PG probes after H_2O_2 treatment display good colocalization with the red mCherry emission of the corresponding SNAP protein target, and the staining pattern can persist for many hours. Because the mitochondrial and ER structures are

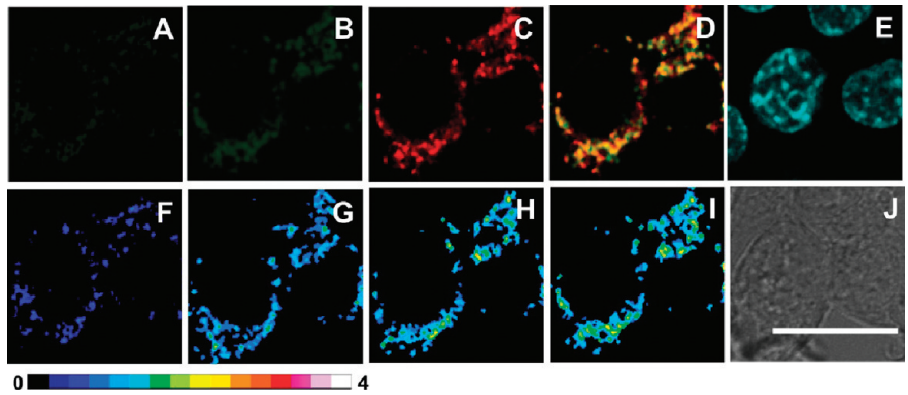

Figure 9. Fluorescence detection of H_2O_2 in living HEK 293T cells transiently expressing SNAP-Cox8A and mCherry-Cox8A. Panels (A) and (B) show fluorescent emission from cells labeled with SPG2 before (A) and after (B) treatment with 100 μM H_2O_2 for 30 min (λ_{exc} = 488 nm, λ_{em} = 500−550 nm), panel (C) presents emission from mCherry-Cox8A, panel (D) displays the overlay of (B) and (C), panel (E) shows nuclear staining with Hoechst 33342, and panels (F−I) display pseudocolor fluorescent emission at 0, 10, 20, and 30 min after addition of 100 μM H_2O_2. Panel (J) presents the brightfield image of cells in (I). Scale bar = 20 μm.

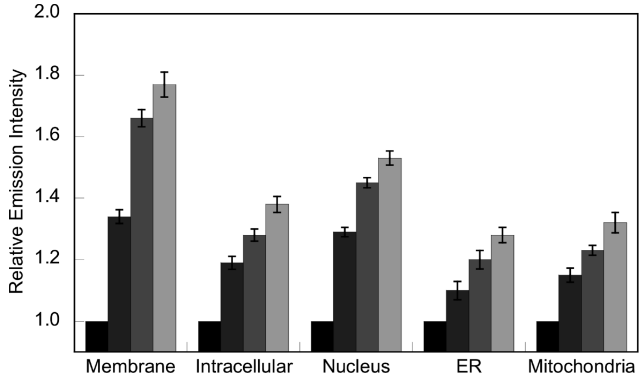

Figure 10. Relative fluorescence emission from time-lapse confocal images of SPG1 or SPG2 labeled HEK 293T cells in response to added 100 μM H_2O_2 at 0, 10, 20, 30 min. Error bars represent standard error of the mean of five experiments.

relatively small compared to the overall volume of the cell, fluorescence emission from these organelles could be easily overwhelmed by noise from any nonspecific staining in cytoplasm. These experiments clearly demonstrate that nonspecific binding is not an issue with the SPG2 probe, as unbound dye can be effectively removed from cells with a simple washing step. Taken together, these data show that SPG1 and SPG2 can be used to label and sense changes in H_2O_2 levels in specific subcellular compartments via selective bioconjugation with a variety of localizable SNAP-tag fusion constructs (Figure 10).

Concluding Remarks

In summary, we have described the synthesis, spectroscopic properties, H_2O_2 responses, and live-cell imaging applications of a new class of organelle-targeted reporters for cellular H_2O_2. SPG1 and SPG2 combine boronate-caged Tokyo Green derivatives for H_2O_2 detection with SNAP tags for site-specific protein labeling at extracellular and intracellular locations, respectively. When SPG1 and SPG2 are exposed to AGT or an AGT fusion protein, these dyes form covalent AGT-PG adducts that respond to H_2O_2 by a turn-on fluorescence increase upon H_2O_2-mediated boronate deprotection. These hybrid small-molecule/protein reporters can be used to label a variety of subcellular locations, including the plasma membrane, nucleus, mitochondria, and endoplasmic reticulum, and detect changes in local H_2O_2 fluxes in living cells by confocal microscopy. The methodology presented here combines the precision of site-specific labeling using genetically encodable tags with the chemical versatility of small-molecule probes. Ongoing efforts are focused on expanding the expanding color palette of targetable H_2O_2 probes, optimizing their sensitivities and dynamic turn-on responses to H_2O_2, creating targetable reporters with ratiometric readouts, and developing additional labeling methodologies for multichannel imaging. We anticipate that simultaneous measurements of H_2O_2 and other ROS fluxes in multiple locales using hybrid small-molecule/protein conjugates will contribute to a better understanding of oxidation biology in states of health, aging, and disease, with particular interest in elucidating cellular redox regulation and signaling in multiple cellular compartments.

Experimental Section

Materials and Methods. All reactions were carried out under a dry nitrogen atmosphere. Silica gel 60 (230−400 mesh, Silicycle) was used for column chromatography. Palladium(II) acetate [$Pd(OAc)_2$], dichloro[1,1′-bis(diphenylphosphino)ferrocene]-palladium(II) [$Pd(dppf)Cl_2$], and 2-(dicyclohexylphosphino)biphenyl [cyclohexyl JohnPhos] were purchased from Strem Chemicals (Newburyport, MA). Bis(pinacolato)diboron was purchased from Boron Molecular (Research Triangle Park, NC). 2,2,2-Trifluoro-N-(4hydroxylmethyl-benzyl)-acetamide (**1**) and O6-(4-Amino-methyl-benzyl)guanine (**4**) were synthesized following literature procedures.[58] All other chemicals were purchased from Sigma-Aldrich (St. Louis, MO) and were used as received. ^{1}H NMR and ^{13}C NMR spectra were collected in $CDCl_3$, DMSO-d_6, or CD_3OD (Cambridge Isotope Laboratories, Cambridge, MA) at 25 °C using a Bruker AVQ-400 spectrometer at the College of Chemistry NMR Facility at the University of California, Berkeley. All chemical shifts are reported in the standard δ notation of parts per million. Low-resolution mass spectral analyses were carried out using GC-MS (Agilent Technology 5975C, inert MSD with triple axis detector) or LC-MS (Agilent Technology 6130, Quadrupole LC/MS). High-resolution mass spectral analyses (ESI-MS, FAB-MS) were carried out at the College of Chemistry Mass Spectrometry Facility at the University of California, Berkeley.

Restiction endonucleases and T4 DNA ligases were purchased from New England Biolabs (Ipswich, MA). Hoechst 33342, monoclonal ANTI-FLAG M2, antibody and Alexa Fluor 488 Goat antimouse lgG antibody were obtained from Invitrogen (Carlsbad, CA). pCEMS-CLIP10m-NK1R, pSEMS-SNAP26m-ADBR, pCEMS1-H2B-CLIP10m, and pSEMS1-Cox8A-SNAP26m plasmids were purchased from Covalys Biosciences (Witterswil, Switzerland). pmCherry and DsRed Golgi were obtained from Clontech Laboratories (Mountain View, CA). pET28a(+) was obtained from

Novagen (EMD Chemicals, Gibbstown, NJ). Primers for PCR amplification were synthesized by Intergrated DNA Technologies (San Diego, CA).

***N*-(4-((2-Amino-6-chloropyrimidin-4-yloxy)methyl)benzyl)-2,2,2-trifluoroacetamide (2).** Compound **1** (1.0 g, 4.3 mmol) in anhydrous DMF (7 mL) was added to a dry 50 mL Schlenk flask under a nitrogen atmosphere. NaH (60% in mineral oil, 515 mg, 12.8 mmol) was then added slowly to the reaction flask. After stirring at room temperature for 15 min, the solution appeared blue-green in color. A solution of 4,6-dichloropyrimidin-4-amine (700 mg, 4.3 mmol) in anhydrous DMF (5 mL) was added dropwise to the reaction flask over a 5 min period, giving a brown-colored solution. The reaction was then heated to 90 °C for 6 h. The reaction was cooled to room temperature, quenched with slow addition of cold water (20 mL), extracted with EtOAc (3 × 30 mL), and dried over Na_2SO_4. Purification by column chromatography (silica gel, EtOAc:hexanes 2:1) gave **2** as a clear viscous oil (300 mg, 19% yield). ^{1}H NMR (DMSO-d_6, 400 MHz): δ 9.99 (1H, br-s), 7.39 (2H, d, J = 8.4 Hz), 7.26 (2H, d, J = 8.4 Hz), 7.09 (2H, s), 6.10 (1H, s), 5.26 (2H, s), 4.36 (2H, s). GC-MS: calculated for [M^+] 360, found 360.

4(4-(Aminomethyl)benzyloxy)-6-chloropyrimidin-2-amine (3). Methylamine (33% in EtOH, 2.5 mL) was added to the solution of **2** (250 mg, 0.69 mmol) in MeOH (5 mL). The mixture was stirred at room temperature for 24 h. The solvent was removed in vacuo, providing product **3** as a white powder (175 mg, 95% yield) ^{1}H NMR (DMSO-d_6, 400 MHz): δ 7.33 (2H, d, J = 8.0 Hz), 7.31 (2H, d, J = 8.0 Hz), 7.10 (2H, br-s), 6.10 (1H, s), 5.25 (2H, s), 3.68 (2H, s) LC-MS: calculated for [M^+] 265.1, found 265.1.

6-Hydroxy-9-(4-hydroxy-2-methylphenyl)-3H-xanthen-3-one (6). Tokyo Green **5** (6.3 g, 18.9 mmol) was added to a dried 500 mL round-bottom flask. Anhydrous CH_2Cl_2 (300 mL) was added by cannula and the resulting insoluble mixture stirred at room temperature for 5 min. The flask was cooled to −78 °C in a CO_2(s)/acetone bath and boron tribromide (14.2 g, 5.4 mL, 56.7 mmol) was added dropwise over 15 min. The reaction was allowed to warm to room temperature overnight and added slowly to 500 mL of vigorously stirred ice/H_2O slurry, causing precipitation of a reddish orange solid. The mixture was stirred for an additional 24 h and the solid collected by vacuum filtration. Purification by flash column chromatography (silica gel, MeOH:CH_2Cl_2 1:10) afforded **4** as a brick red solid (5.3 g, 87% yield). ^{1}H NMR (DMSO-d_6, 400 MHz): δ 10.00 (1H, s), 7.35 (2H, d, J = 9.2 Hz), 7.08 (2H, d, J = 8.0 Hz), 7.07 (1H, s), 7.03 (2H, dd, J = 9.2, 2.4), 6.87 (1H, d, J = 2.4 Hz), 6.83 (2H, dd, J = 8.0, 2.4), 1.90 (3H, s). LC-MS: calculated for [MH^+] 319, found 319.

***tert*-Butyl 2-(4-(6-hydroxy-3-oxo-3H-xanthen-9-yl)-3-methylphenoxy)acetate (7).** Phenolic TG **6** (3.13 g, 10.0 mmol) was added to a dried 500 mL Schlenk flask. Anhydrous DMF (300 mL) and cesium carbonate (22.2 g, 68.1 mmol) were added, and the mixture stirred at room temperature for 60 min. *tert*-Butylbromoacetate (1.95 g, 1.46 mL, 10.0 mmol) was added by micropipettor and the resulting reaction mixture stirred at room temperature overnight. The reaction was filtered and solvent concentrated under reduced pressure, giving a dark brown mass. H_2O (100 mL) was added and the solution neutralized with 1 M HCl, giving a red orange precipitate. The solid was collected by vacuum filtration, washed with H_2O (100 mL), and dried in air. Purification by flash column chromatography (silica gel, MeOH:CH_2Cl_2 1:20) furnished **5** as a brick red solid (1.54 g, 36% yield). ^{1}H NMR ($CDCl_3$, 400 MHz): δ 7.10 (2H, d, J = 9.2 Hz), 7.09 (1H, d, J = 8.4 Hz), 6.93 (1H, d, J = 2.4 Hz), 6.89 (1H, s), 6.88 (2H, s), 6.83 (2H, dd, J = 9.2, 2.4 Hz), 4.61 (2H, s), 2.03 (3H, s), 1.54 (9H, s). LC-MS: calculated for [MH^+] 433, found 433.

***tert*-Butyl-2-(3-methyl-4-(3-oxo-6-(trifluoromethylsulfonyloxy)-3H-xanthen-9-yl)phenoxy)acetate (8).** *tert*-Butyl TG **7** (1.06 g, 2.44 mmol) was added to a dried 25 mL Schlenk flask. Anhydrous DMF (5 mL) and DIPEA (1.57 g, 2.1 mL, 12.2 mmol) were added, and the resulting mixture stirred at room temperature for 60 min. *N*-Phenyl bis-trifluoromethane sulfonimide (1.37 g, 3.84 mmol) was dissolved in anhydrous DMF (3 mL) and added dropwise to the stirring basic solution over 5 min. The mixture was stirred at room temperature overnight, diluted in toluene (200 mL), washed with H_2O (3 × 100 mL), and dried over $MgSO_4$. Purification by flash column chromatography (silica gel, EtOAc:hexanes 1:4 to 1:2 gradient) gave **8** as a puffy, orange crystalline solid (930 mg, 67% yield). ^{1}H NMR ($CDCl_3$, 400 MHz): δ 7.39 (1H, d, J = 2.4 Hz), 7.18 (1H, d, J = 8.8 Hz), 7.09 (2H, d, J = 8.8, 2.4 Hz), 7.01 (1H, d, J = 10.0 Hz), 6.95 (1H, d, J = 2.4 Hz), 6.91 (1H, dd, J = 10, 2.4 Hz), 6.60 (1H, dd, J = 10.0 2.0 Hz), 6.44 (1H, d, J = 2.0 Hz), 4.61 (2H, s), 2.05 (3H, s), 1.54 (9H, s). LC-MS: calculated for [MH^+] 565, found 565.

***tert*-Butyl-2-(3-methyl-4-(3-oxo-6-(4,4,5,5-tetramethyl-1,3,2-dioxaborolan-2-yl)-3H-xanthen-9-yl)phenoxy)acetate (9).** Compound **8** (641 mg, 1.14 mmol), $Pd(OAc)_2$ (84 mg, 0.12 mmol), cyclohexyl JohnPhos (201 mg, 0.57 mmol), and bis(pinacolato)diboron (446 mg, 1.76 mmol) were added to a dried 25 mL scintillation vial in a glovebox. Anhydrous 1,4-dioxane (10 mL) was added and the solution stirred at room temperature for 5 min. Anhydrous DIPEA (742 mg, 1.00 mL, 5.74 mmol) was added dropwise by syringe and the reaction mixture was stirred at room temperature overnight. The reaction vial was removed from the glovebox, poured into saturated aqueous NH_4Cl (30 mL), extracted with EtOAc (3 × 30 mL), and dried over $MgSO_4$. Purification by flash column chromatography (silica gel, EtOAc:hexanes 1:4) delivered **9** as an orange crystalline solid (615 mg, 99% yield). ^{1}H NMR ($CDCl_3$, 400 MHz): δ 7.90 (1H, s), 7.57 (1H, d, J = 8.0 Hz), 7.08 (1H, J = 8.4 Hz), 7.07 (1H, d, J = 8.0 Hz), 7.01 (1H, d, J = 9.6 Hz), 6.94 (1H, d, J = 2.4 Hz), 6.89 (1H, dd, J = 8.4, 2.4 Hz), 6.59 (1H, dd, J = 9.6, 2.0 Hz) 6.43 (1H, d, J = 2.0 Hz), 4.61 (2H, s), 2.03 (3H, s), 1.54 (9H, s), 1.37 (12H, s). LC-MS: calculated for [MH^+] 543, found 543.

2-(3-Methyl-4-(3-oxo-6-(4,4,5,5-tetramethyl-1,3,2-dioxaborolan-2-yl)-3H-xanthen-9-yl)phenoxy)acetic acid (10). *tert*-Butyl PG **9** (542 mg, 1.0 mmol) was dissolved in CH_2Cl_2 (3 mL) and added dropwise by Pasteur pipet to a stirring mixture of CH_2Cl_2:TFA (1.0:1.0, 25 mL). The solution was allowed to stir for 4 h and the solvent removed under reduced pressure. Purification by flash column chromatography (silica gel, MeOH:CH_2Cl_2 1:10) gave **10** as an orange film (419 mg, 86% yield). ^{1}H NMR ($CDCl_3$, 400 MHz): δ 8.23 (1H, s), 7.82 (1H, d, J = 8.0 Hz), 7.41 (1H, d, J = 8.0 Hz), 7.40 (1H, d, J = 8.8 Hz) 7.15 (3H, m), 7.04 (1H, s), 7.00 (1H, d, J = 8.8 Hz), 4.83 (2H, s), 2.01 (3H, s), 1.39 (12H, s). LC-MS: calculated for [MH^+] 487, found 487.

***N*-(4-((2-Amino-9*H*-purin-6-yloxy)methyl)benzyl)-2-(3-methyl-4-(3-oxo-6-(4,4,5,5-tetramethyl-1,3,2-dioxaborolan-2-yl)-3H-xanthen-9-yl)phenoxy)acetamide, SPG1 (11).** Compound **10** (99 mg, 0.20 mmol) was added to a dried 25 mL Schlenk flask. Anhydrous DMF (3 mL) was added by syringe and the solution was stirred at room temperature for 5 min. HATU (89 mg, 0.23 mmol), 6-(4-(aminomethyl)benzyloxy)-9*H*-purin-2-amine **4** (63 mg, 0.23 mmol), and DIPEA (266 mg, 0.359 mL, 2.06 mmol) were added, and the reaction stirred at room temperature overnight. The reaction was poured into an ice/H_2O slurry (30 mL) and stirred to precipitate an orange solid. The solid was collected by vacuum filtration and dried in vacuo. Purification by flash column chromatography (silica gel, MeOH:CH_2Cl_2 1:10) provided SPG1 **11** as an orange film (17.1 mg, 11% yield). ^{1}H NMR (DMSO-d_6, 400 MHz): δ 12.41 (1H, s), 8.75 (1H, s), 7.78 (1H, s), 7.71 (1H, s), 7.55 (1H, d, J = 7.6 Hz), 7.45 (2H, d, J = 7.2 Hz) 7.31 (2H, d, J = 7.6 Hz), 7.24 (1H, d, J = 8.4 Hz), 7.11 (1H, s), 7.04 (2H, d, J = 8.4 Hz), 6.94 (1H, d, J = 9.6 Hz), 6.50 (1H, d, J = 9.6 Hz), 6.29 (2H, s), 6.25 (1H, s), 5.44 (2H, s), 4.67 (2H, s), 4.39 (2H, d, J = 6.4 Hz), 1.98 (3H, s), 1.31 (12H, s). HRFAB-MS: calculated for [MH^+] 739.3042, found 739.3046.

***N*-(4-((2-Amino-6-chloropyrimidin-4-yloxy)methyl)benzyl)-2-(3-methyl-4-(3-oxo-6-(4,4,5,5-tetramethyl-1,3,2-dioxaborolan-2-yl)-3*H*-xanthen-9-yl)phenoxy)acetamide, SPG2 (12).** Compound **10** (25 mg, 0.051 mmol) dissolved in anhydrous DMF (2 mL) was added

to a dried 5 mL round-bottom flask and the solution was stirred at room temperature for 5 min. HATU (25 mg, 0.066 mmol), compound **3** (18 mg, 0.068 mmol), and DIPEA (25 uL) were added, and the reaction was stirred at room temperature overnight. DMF was removed under vacuo and the orange oil was redissolved in 10% MeOH in CH_2Cl_2. Purification by flash column chromatography (silica gel, MeOH:CH_2Cl_2 1:10) afforded SPG2 **12** as an orange film (20 mg, 0.027 mmol, 53% yield). ^{1}H NMR (20% MeOD in $CDCl_3$) δ 7.92 (1H, s), 7.55 (1H, d, $J = 6.4$ Hz), 7.33 (2H, d, $J = 6.4$ Hz), 7.28 (2H, d, $J = 6.4$ Hz), 7.07 (1H, d, $J = 6.8$ Hz), 7.02 (1H, d, $J = 6.4$ Hz), 6.90−7.00 (3H, m), 6.58 (1H, d, $J = 7.6$ Hz), 6.43 (1H, s), 6.06 (1H, s), 5.26 (2H, s), 4.61 (2H, s), 4.53 (2H, d, $J = 3.6$ Hz), 1.98 (3H, s), 1.32 (12H, s). ESI-MS: calculated for [MH$^+$] 733.25, found 733.26.

2-(4-(6-Hydroxy-3-oxo-3H-xanthen-9-yl)-3-methylphenoxy)acetic acid (13). Compound **7** (200 mg, 0.46 mmol) was stirred in a mixture of CH_2Cl_2:TFA (1:2, 20 mL) for 1 h. Removal of the solvent under vacuum gave a viscous orange oil. EtOAc (10 mL) was added, and the mixture was sonicated for 30 min. Slow addition of the EtOAc mixture into a beaker of vigorously stirring hexane (30 mL) gave carboxyl TG **13** as orange solid precipitate (120 mg, 0.32 mmol, 69% yield). ^{1}H NMR (CD_3OD, 400 MHz) δ 7.32 (2H, d, $J = 8.6$ Hz), 7.19 (1H, d, $J = 8.4$ Hz), 7.08 (1H, d, $J = 2.0$ Hz), 7.03 (1H, dd, $J = 8.4$, 2.0 Hz), 6.96 (2H, s), 6.92 (2H, d, $J = 8.6$ Hz), 4.80 (2H, s), 1.97 (3H, s). LC-MS: calculated for [MH$^+$] 377.1, found 377.0.

***N*-(4-((2-Amino-9*H*-purin-6-yloxy)methyl)benzyl)-2-(4-(6-hydroxy-3-oxo-3*H*-xanthen-9-yl)-3-methylphenoxy)acetamide, SNAP-TG1 (14).** Compound **13** (235 mg, 0.67 mmol) was added to a dried 25 mL Schlenk flask. Anhydrous DMF (5 mL) was added by syringe and the solution was stirred at room temperature for 5 min. HATU (256 mg, 0.67 mmol), 6-(4-(aminomethyl)benzyloxy)-9*H*-purin-2-amine **4** (182 mg, 0.67 mmol), and DIPEA (0.87 mL) were added, and the reaction stirred at room temperature overnight. The reaction was poured into an ice/H_2O slurry (30 mL) and stirred to precipitate an orange solid. The solid was collected by vacuum filtration and dried *in vacuo*. Purification by flash column chromatography (silica gel, MeOH:CH_2Cl_2 1:10) delivered STG1 **14** as an orange solid (197 mg, 0.31 mmol, 46% yield). ^{1}H NMR (DMSO-d_6, 400 MHz) δ 12.42 (1H, br-s), 8.74 (1H, s), 7.82 (1H, s), 7.45 (2H, d, $J = 7.2$ Hz), 7.29 (2H, d, $J = 7.2$ Hz), 7.20 (1H, d, $J = 8.4$ Hz), 7.09 (1H, s), 7.02 (1H, d, $J = 8.0$ Hz), 6.87 (2H, d, $J = 8.8$ Hz), 6.50−6.80 (4H, m), 6.29 (2H, br s), 5.44 (2H, s), 4.66 (2H, s), 4.38 (2H, d, $J = 5.2$ Hz), 3.16 (1H, s), 1.98 (3H, s). ESI-MS: calculated for [MH$^+$] 629.21, found 629.21.

***N*-(3-((2-Amino-6-chloropyrimidin-4-yloxy)methyl)benzyl)-2-(4-(6-hydroxy-3-oxo-3*H*-xanthen-9-yl)-3-methylphenoxy)acetamide, STG2 (15).** Compound **13** (30 mg, 0.079 mmol) in anhydrous DMF (2 mL) and HATU (30 mg, 0.078 mmol) were added to a dried 5 mL round-bottom flask and the solution was stirred at room temperature for 5 min. Compound **3** (21 mg, 0.079 mmol), and DIPEA (100 μL) were added, and the reaction was stirred at room temperature overnight. DMF was removed *in vacuo*, and the orange oil was redissolved in 10% MeOH in CH_2Cl_2. Purification by flash column chromatography (silica gel, MeOH:CH_2Cl_2 1:10) afforded STG2 **15** as an orange film (45 mg, 0.072 mmol, 91% yield). ^{1}H NMR (20% CD_3OD in $CDCl_3$) δ 7.35 (1H, t, $J = 6.0$ Hz), 7.25 (2H, d, $J = 8.2$), 7.21 (2H, $J = 8.2$ Hz), 6.98 (1H, d, $J = 8.0$), 6.91 (2H, d, $J = 8.8$ Hz), 6.85 (1H, s), 6.82 (1H, d, $J = 8.0$), 6.41 (2H, d, $J = 2.0$ Hz), 6.60 (2H, dd, $J = 8.8$, 2.0 Hz), 5.97 (1H, s), 5.16 (2H, s), 4.52 (2H, s), 4.44 (2H, d, $J = 6.0$ Hz), 1.97 (3H, s) ESI-MS: calculated for [MH$^+$] 623.16, found 623.17.

Expression and Purification of His-AGT for SNAP Labeling. The sequence encoding SNAP was PCR amplifed from pSEMS-SNAP-ADBR (Covalys) and subcloned into PET28a(+) (Novagen) using NheI/XhoI restriction sites. The resulting plasmid, after verified by DNA sequencing, was transformed into *E. coli* strain BL-21(DE3). A bacterial culture was grown at 37 °C in TB medium (50 mL) with 50 μg/mL Kanamycin for 6−8 h until an optical density (OD_{600nm}) of 0.8 was reached. Expression of His-AGT was induced by addition of 0.5 mM isopropyl-β-D-thiogalactopyranoside (IPTG). The culture was grown at 16 °C for 12 h and was harvested by centrifugation at 8000 rpm for 10 min at 4 °C. Cell lysates were prepared by resuspending the pellet in buffer (PBS with 0.5 mM phenylmethylsulfonyl fluoride) followed by FRENCH press (Thermo Scientific). Insoluble protein and cell debris were removed by centrifugation at 10000 rpm for 30 min. For purification of His-AGT, Ni-NTA (Qiagen) was used according to the supplier's protocol. The fractions with His-AGT were combined and concentrated using an Amicon Ultra-15 Ultracel-10K centrifugal unit (Millipore). The concentrated His-AGT solution was then desalted using G25 Sephadex (Sigma Aldrich) with the following elution buffer: 150 mM NaCl, 25 mM Tris-Cl, 1 mM DTT pH 7.5. The purified His-AGT protein was concentrated using an Amicon Ultra-4 Ultracel-10K and stored at −20 °C. The protein concentration was determined using the BCA assay, yielding 8.6 mg of purified His-AGT (1.5 mM in 250 μL elution buffer).

In Vitro SNAP Labeling and Analysis by ESI-MS and In-Gel Fluorescence Scanning. Purified His-AGT (0.5 uM) was incubated in reaction buffer (PBS pH 7.4, 1 mM DTT) at 37 °C with 0.5 μM of either SPG1, SPG2, STG1, or STG2 for 30 min at 37 °C. Binding of the fluorescent dyes to His-AGT was analyzed by SDS-PAGE, followed by in-gel fluorescence scanning (488 nm Argon excitation, 520 BP 40 emission filter, Typhoon 9410 imaging system, GE Healthcare) and Coomassie protein staining. For mass spectrometric analysis and spectroscopic measurements, His-AGT (1 μM) was incubated in 20 mM HEPES buffer pH 7 (1 mL) with 5 μM of either SPG1, SPG2, STG1, or STG2 for 30 min at 37 °C. The reaction was concentrated to 50 μM with an Amicon 4 10K column (Milipore) and subjected to size-exclusive gel filtration with Bio-Rad Micro Bio-Spin 6 chromatography column to remove the excess dye. The deconvoluted MS data were collected by Dr. Anthony T. Iavarone at UC Berkeley QB3 Mass Spectrometry Facility.

Spectroscopic Materials and Methods. Millipore water was used to prepare all aqueous solutions. All spectroscopic measurements were performed in 20 mM HEPES buffer, pH 7.0, 25 °C. Absorption spectra were recorded using a Varian Cary 50 spectrophotometer (Walnut Creek, CA). Fluorescence spectra were recorded using a Photon Technology International Quanta Master 4 L-format scanning spectrofluorometer (Lawrenceville, NJ) equipped with an LPS-220B 75-W xenon lamp and power supply, A-1010B lamp housing with integrated igniter, switchable 814 photon-counting/analog photomultiplier detection unit, and MD5020 motor driver. Samples for absorption and fluorescence measurements were contained in 1-cm × 1-cm quartz cuvettes (1.4 mL volume, Starna, Atascadero, CA). Fluorescein in 0.1 M NaOH ($\Phi = 0.85$)[90] was used as standard for quantum yield measurements.

Cell Culture and Labeling Procedures. HEK 293T cells were cultured in DMEM (Invitrogen) supplemented with 10% fetal bovine serum (FBS, Hyclone) and glutamine (2 mM). One day before transfection, cells were passaged and plated on 4-wells Lab-Tek borosilicate chambered coverglass (Nunc). Transient expression of SNAP fusion protein or mCherry was performed by following the standard protocol of Lipofectamine 2000. SNAP-tag labeling was achieved by incubating cells in DPBS containing 5 μM dye and 1 μM Hoechst 33342 for 30 min at 37 °C. For membrane labeling with cell-impermeable SPG1 or STG1, cells were washed with fresh DPBS (2 × 1 mL) before image acquisition. Labeling of intracellular targets with STG2 or SPG2 required incubation of cells in fresh DMEM with 10% FBS (2 × 1 mL) for 30 min after dye loading to remove any unbound fluorophore. All confocal fluorescence images were acquired in DPBS media.

Fluorescence Imaging Experiments. Confocal fluorescence imaging studies were performed with a Zeiss LSM510 NLO Axiovert 200 Laser scanning microscope and a 40× oil-immersion

(90) Parker, C. A.; Rees, W. T. *Analyst* **1960**, *85*, 587–600.

objective lens. The motorized stage on the microscope was equipped with an incubator, maintaining the sample at 37 °C in a 5% CO_2 humidified atmosphere. Excitation of the SNAP tag probe at 488 nm was carried out with an argon laser and emission was collected using a 500−550 nm filter. Excitation of mCherry was carried out with a helium−neon 543 nm laser and emission was collected using a LP560 filter. Excitation of Hoechst 33342 was carried out using a MaiTai two-photon laser at 770 nm pulses (mode-locked Ti:sapphire laser, Tsunami Spectra Physics) and emission was collected through 385−425 nm filter. Image analysis was performed in ImageJ (National Institute of Health).

Acknowledgment. We thank the Packard and Sloan Foundations, the Hellman Faculty Fund (UC Berkeley), Amgen, Astra Zeneca, and the National Institute of General Medical Sciences (NIH GM 79465) for funding this work. C.J.C. is an Investigator with the Howard Hughes Medical Institute. D.S. was supported by a scholarship from the Ministry of Science, Thailand. A.E.A. thanks the NIH Chemical Biology Graduate Program (T32 GM066698) for support, as well as the ACS Organic Division for an Emmanuil Troyansky Graduate Fellowship and UC Berkeley for a Chancellor's Opportunity Fellowship. We thank Holly Aaron (UCB Molecular Imaging Center), Ann Fischer (UCB Tissue Culture Facility), and Prof. Michelle Chang (UCB Department of Chemistry) for expert technical assistance and helpful discussions.

Supporting Information Available: Mass spectrometry and in-gel fluorescence analysis of intact AGT as well as AGT-PG and AGT-TG adducts, details of construction of plasmids, and complete ref 54. This material is available free of charge via the Internet at http://pubs.acs.org.

JA100117U